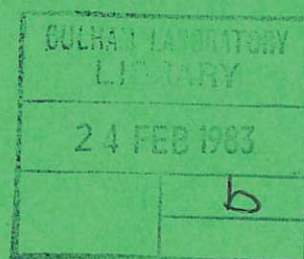




UKAEA

Preprint



THE PLASMA BOUNDARY REGION AND THE ROLE OF ATOMIC AND MOLECULAR PROCESSES

M. F. A. HARRISON

CULHAM LABORATORY
Abingdon Oxfordshire

1982

This document is intended for publication in a journal or at a conference and is made available on the understanding that extracts or references will not be published prior to publication of the original, without the consent of the authors.

Enquiries about copyright and reproduction should be addressed to the Librarian, UKAEA, Culham Laboratory, Abingdon, Oxon. OX14 3DB, England.

THE PLASMA BOUNDARY REGION AND THE ROLE OF ATOMIC AND MOLECULAR PROCESSES

(A series of four lectures presented at the NATO Advanced Study Institute on Atomic and Molecular Processes in Controlled Thermonuclear Fusion; Palermo, July 1982)

M F A Harrison

Culham Laboratory, Abingdon, Oxon OX14 3DB, UK
(Euratom/UKAEA Fusion Association)

ABSTRACT

Confinement of plasma particles and energy by a magnetic field is degraded in a region close to the wall of the containment vessel due to localised processes which give rise to enhanced losses of charge particles and energy. Losses arise due to the contact of energetic plasma with the vessel wall and, in the case of fusion devices, the principal constituents of the plasma are electrons, deuterons and tritons. Interaction of plasma with the wall causes the release of neutral "hydrogen" and also of impurity elements such as sputtered atoms of the wall material. Electrons and "protons" in the plasma collide with the particles which are released from the wall and a complex sequence of atomic processes is established which embraces ionisation, photon emission and the formation of daughter atoms by charge exchange. These and other atomic processes contribute to the loss of energy and particles in the locality of the wall and they also act as coupling mechanisms between plasma and surface interactions.

The boundary region is somewhat indeterminate but, for the basis of the present discussion, it is assumed to be defined as that part of the plasma where plasma transport is predominantly in the direction of the magnetic field. Moreover, the discussion is restricted to toroidal confinement devices and, because of the breadth of existing studies, particular emphasis is placed upon the tokamak configuration.

The objective of this paper is to describe in outline the basic processes of plasma transport and plasma surface interactions and to consider the relevance of atomic processes in the specific environment of the boundary region. Incorporation of these basic processes into self-consistent models of the boundary region will be briefly described and some examples will be given of the boundary conditions predicted.

July 1982

1. INTRODUCTION

Confinement of plasma particles and energy by a magnetic field is degraded in a region close to the wall of the containment vessel due to localised processes which give rise to enhanced losses of charged particles and energy. Losses of thermal energy occur when the magnetic field lines intercept the wall of the vessel and also because plasma ion bombardment of the wall releases radiating impurity elements due to processes such as sputtering. Neutralisation of plasma ions* in collisions with the wall is the principal source of neutral atoms within the vessel and subsequent charge exchange of these atoms with ions in the adjacent plasma provides a mechanism by which energetic neutral particles can cross the magnetic field and thereby recycle between the plasma and the wall. This recycling of energetic atoms is a source of energy loss from the plasma and also an additional mechanism for the release of impurity elements. Thus the concentration of neutralised plasma ions and also of impurity atoms and ions is peaked close to the wall where inelastic atomic collisions between electrons and these atomic species result in localised cooling of the plasma electrons. The principal cooling processes are excitation followed by spontaneous emission of photons which are absorbed by the wall. In addition, ionisation yields cold secondary electrons and thereby reduces the average temperature of the plasma.

The boundary region is somewhat indeterminate but for the basis of the present discussion it will be assumed that it can be defined as that part of the plasma where plasma transport is predominantly in the direction of the magnetic field. This implies that the magnetic flux tubes in the boundary must intercept the walls of the vessel and so these magnetic field lines are termed "open". The interface between the boundary region and the confined plasma therefore occurs at the "separatrix". This is the magnetic surface that bounds the region wherein the field lines are "closed" so that plasma transport towards the wall must take place by motion across the magnetic field. For the sake of conciseness the subsequent discussion will be restricted to toroidal confinement devices and, because of the breadth of existing studies, particular emphasis will be placed upon the tokamak configuration.

*Plasma ions in fusion research are predominantly protons whose neutralised products are thus either "hydrogen" atoms or molecules. The plasma in a DT fusion reactor will be formed from deuterium and tritium but these species will be referred to here as "hydrogen" unless a distinction must be made between the isotopes.

Plasma behaviour in the boundary region plays a major role in determining the rate of build-up and the ultimate steady state concentration of impurity ions within the confined plasma. Control of this impurity concentration will be a particularly important factor in near term experiments such as TFTR and JET where the plasma heating period will extend for several seconds. Recycling of neutral particles within the boundary influences strongly the ability of external vacuum pumps to exhaust neutral gas from the edge of the plasma and, since the plasma in longer term devices such as INTOR¹ must ignite and burn for 100 to 200 s, it will be necessary not only to control impurities but also to fuel with neutral DT and to exhaust the helium gas produced from the $^3\text{D} + ^3\text{T} \rightarrow ^4\text{He} + \text{n}$ fusion reaction. These requirements have, during recent years, provided a stimulus for developing self-consistent concepts of the boundary plasma in which the interactive mechanisms of plasma transport are coupled by atomic processes to plasma-surface interactions. By these means it has been possible to evolve self-consistent models of the boundary region which can be used as a design base for next generation devices and also as a means for interpreting present-day experiments.

The objective of this paper is to describe in outline the basic processes of plasma transport and plasma surface interactions and to discuss the atomic processes of particular relevance to the boundary region. Incorporation of these basic processes into self-consistent models of the boundary region will be briefly described and some examples will be given of the boundary conditions predicted. The self-consistent amalgamation of these disparate subjects into a general description of the plasma is a relatively new concept; recent surveys can be found in articles by Post² and Harrison³ and an appreciation of the present status can be gained from the proceedings of specialised conferences such as Ref.4.

2. MAGNETIC TOPOLOGY OF THE PLASMA BOUNDARY

An elemental tube of magnetic flux in the boundary region of a toroidal plasma can be envisaged in the manner indicated in Figure 1(a) where a ribbon-like flux tube is shown wrapped over the separatrix surface. The magnetic field consists of two components; the toroidal field B_{tor} and the poloidal field B_{pol} . In the case of the tokamak, B_{tor} is generated using external windings but B_{pol} is generated by a current that is induced to flow in a toroidal direction within the plasma. The flux tube twists around the torus and the length of a closed tube in the direction z parallel to

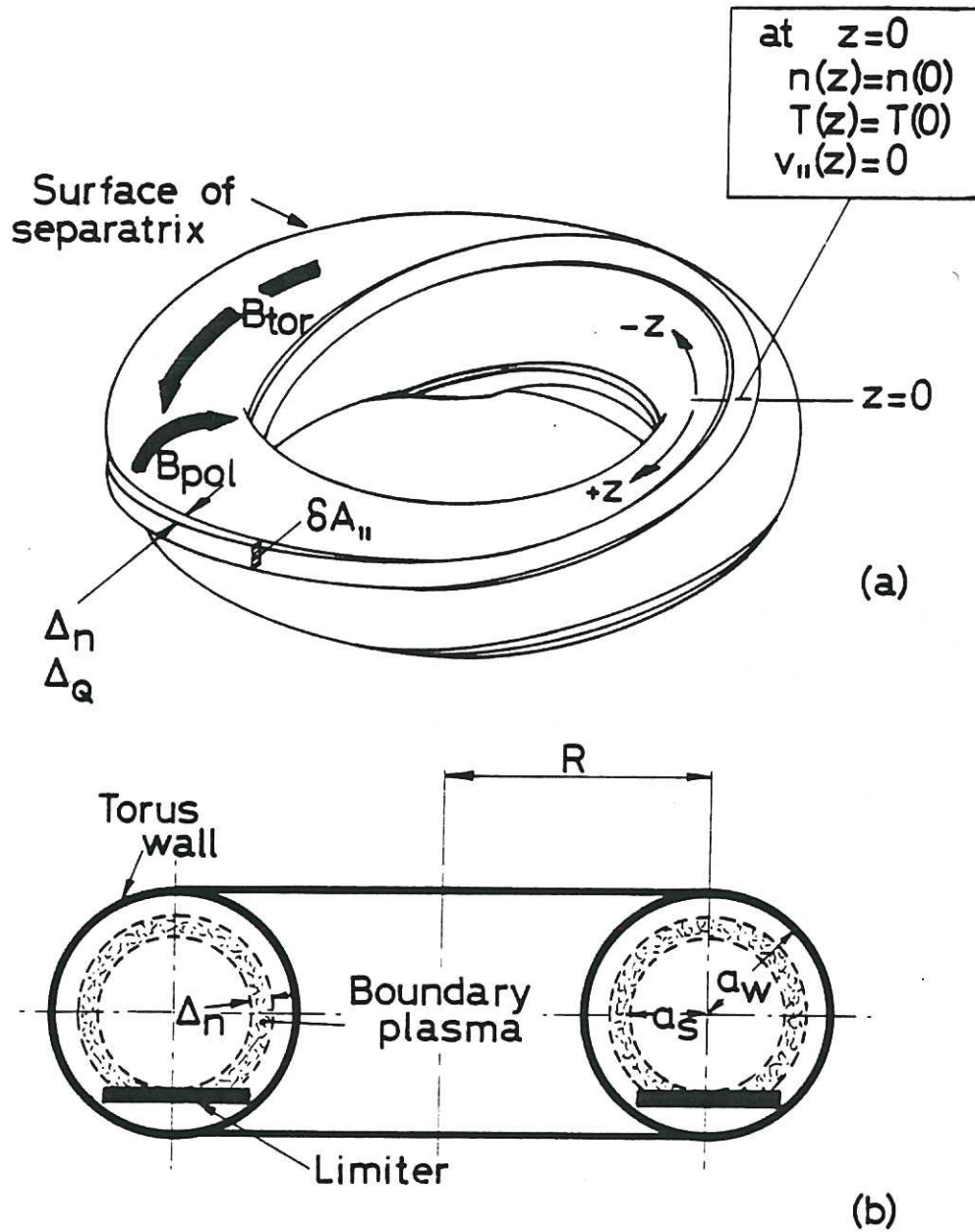


Fig.1 Topology of a conceptual boundary plasma.

(a) shows an elemental tube of magnetic flux. The tube has an area $\delta A_{||}$ normal to the field and its radial extent is either Δ_n or Δ_Q depending upon whether the flow of particles or energy is being considered; the total length of the tube is $2\pi Rq(a_s)$.

(b) shows the boundary plasma associated with a toroidally symmetric limiter plate located at the bottom of the torus. The radial position a_s defines the position of the separatrix.

the resultant magnetic field can be expressed as

$$L_{||} = 2\pi Rq(r) \quad (2.1)$$

where

$$q(r) = \frac{r}{R} \frac{B_{\text{tor}}}{B_{\text{pol}}}$$

is the safety factor of the plasma of major radius R and minor radius r . It is customary to protect the torus wall by a limiter so that the separatrix radius a_s , shown in Figure 1(b), is inboard of the wall radius a_w . At the separatrix, the field lines are open and, since the limiter shown in Figure 1(b) is symmetrical in the toroidal direction, the length of these open lines is

$$L_{||}(a_s) \approx 2\pi Rq(a_s).$$

It is assumed that there is negligible flow of plasma current in the boundary region outboard of the separatrix, so that those plasma electrons and ions that diffuse outward across the separatrix will enter this flux tube with an equal probability of drifting towards the limiter in either the positive or negative direction of z . Thus the average length of boundary flux tube traversed by plasma which flows across the separatrix and then flows to the limiter surface can be taken as

$$\frac{1}{2} L_{||}(a_s) = \pi Rq(a_s). \quad (2.2)$$

The residence time for plasma particles within the boundary can then be expressed as

$$\tau_{||} = \frac{\pi Rq}{v_{||}} \quad (2.3)$$

where $v_{||}$ is the drift velocity of the plasma along the flux tube. It will be seen in Section 3 that the average drift velocity in the z direction will generally be less than the ion sound speed,

$$C_s = \left(\frac{ZkT_e + kT_i}{m_i} \right)^{1/2}, \quad (2.4)$$

where T_e and T_i are respectively the electron and ion temperatures.*

*Throughout this paper the symbol T is used whenever kT is expressed in eV and in general Gaussian units are used for other parameters. The symbols e , k , etc, have their conventional meaning. The electron and ion masses are m_e and m_i and their temperatures are T_e and T_i . For a DT mixture m_i is taken as $2.5 m_i(\text{proton})$. The ion charge state is denoted by Z .

The particle residence time $\tau_{||}$ is typically $\sim 10^{-3}$ s and it is appreciably shorter than the characteristic time, τ_{\perp} , for plasma particle transport across the magnetic field; τ_{\perp} ranges from $\sim 10^{-2}$ s in present-day experiments to predicted values of ~ 1 s in large devices such as INTOR. Even so, some cross field transport must take place during the time taken for the boundary plasma to drift along the open field lines and the scale length of the radial gradient of plasma density in the boundary can, in its simplest form, be expressed as

$$\Delta_n = (D_{\perp} \tau_{||})^{\frac{1}{2}} \quad (2.5)$$

where D_{\perp} is the diffusion coefficient for cross field diffusion. Typically Δ_n is a few cm.

Particles in the boundary plasma will thus flow in a region that extends a distance $\sim \Delta_n$ outboard of the separatrix and the volume of this boundary region is about $4\pi^2 R a_s \Delta_n$. This volume is filled with flux tubes whose length is $2\pi R q(a_s)$ and so it is convenient to envisage that plasma flows along a channel which comprises a group of elemental flux tubes each of which has a radial thickness Δ_n and elemental area $\delta[A_{||}]_n$ normal to the direction z . The total area of the channel along which plasma particles flow to the limiter is thus given by

$$[A_{||}]_n \approx \frac{4\pi^2 R a_s \Delta_n}{2\pi R q(a_s)} \approx \frac{2\pi a_s \Delta_n}{q(a_s)} \quad (2.6)$$

and, if magnetic flux is conserved, $[A_{||}]_n$ is uniform throughout the length of the flow channel.

3. TRANSPORT TO THE LIMITER SURFACE OF PLASMA PARTICLES AND ENERGY IN THE DIRECTION PARALLEL TO THE MAGNETIC FIELD

The principal characteristics of transport along the magnetic field are conveniently discussed in terms of the linear representation of the flow channel which is illustrated schematically in Figure 2. The face of the channel which lies in contact with the separatrix is assumed to be fed uniformly by the outward flow of particles and of energy that are transported into the boundary plasma by transport across the magnetic field. Within the boundary, plasma flow is predominantly in the positive and negative directions of z and plasma sheaths will be established at the ends of the channel where the plasma is in contact with the limiter surface.

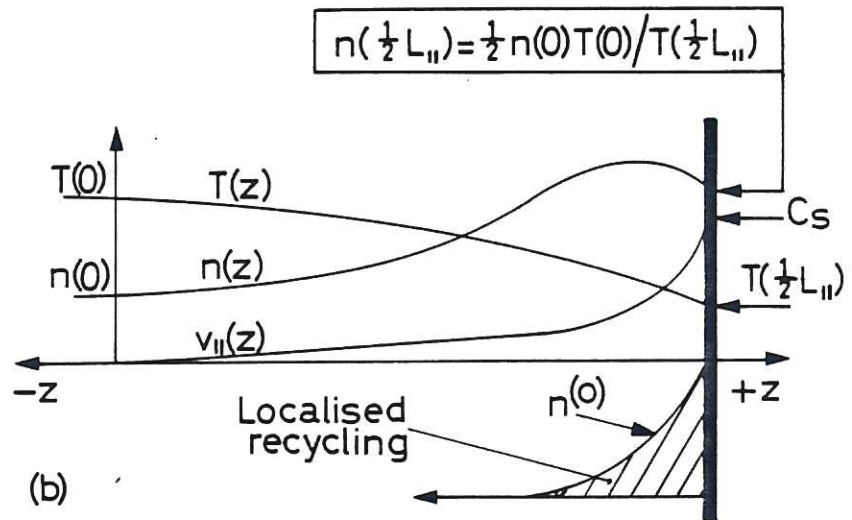
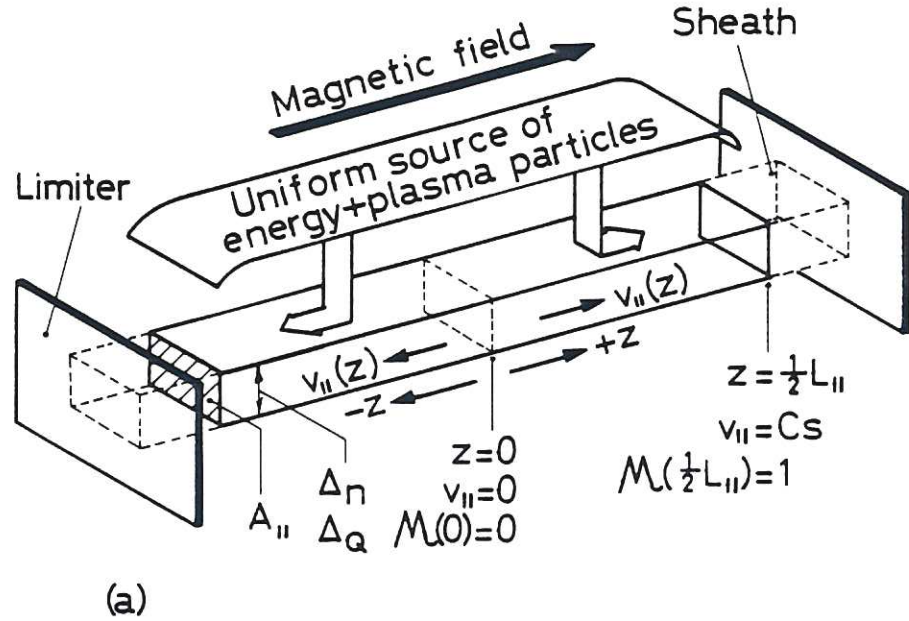


Fig.2 Linear representation of the flow channel for collisional plasma transport along the magnetic field in the boundary region.

(a) shows a simple one-dimensional concept of flow parallel to z which is terminated by plasma sheaths at the surface of a limiter.

(b) shows the dependence upon z of the plasma density, n , temperature, T , and flow velocity $v_{||}$. The conditions sketched refer to powerful recycling in the locality of the limiter; $n^{(o)}$ being the density of neutral particles formed by plasma bombardment of the limiter surface. Sources of charged particles and energy in other regions are assumed to be uniformly distributed in the z direction.

Properties of the plasma sheath

Plasma contained in a vessel with electrically conducting walls will, in the absence of a magnetic field, assume a positive potential with respect to the walls whenever $T_e \gtrsim T_i$. The potential ensures that the ready flow of charge carried by mobile electrons to the wall is reduced (due to the repulsive electrostatic force) so that it equals that carried by ions. This condition is likely to pertain to flow parallel to the magnetic field in the boundary plasma. The nett loss of charge is then zero and an electrostatic field is established in the vicinity of the wall, the extent of this field being related to the screening properties of the plasma. The scale length of the potential gradient is characterised by the Debye screening length, λ_D , which can be expressed as

$$\lambda_D = \left(\frac{kT_e}{4\pi n_e e^2} \right)^{\frac{1}{2}} = 7.43 \times 10^2 \left(\frac{T_e}{n_e} \right)^{\frac{1}{2}} \quad [\text{cm}] \quad (3.1)$$

where n_e is the number density of plasma electrons. The sheath potential U can be determined from Poisson's equation in which are substituted the densities of electrons and ions in the region close to the wall (see for example Chen⁵). A solution,

$$U = \frac{kT_e}{2e} \ln \left(\frac{m_i}{2\pi m_e} \right), \quad (3.2)$$

is representative of singly charged ions that are incident upon a plane surface and uninfluenced by a magnetic field. For a "hydrogen plasma" $U \approx 3T_e/e$.

There is also a longer range, ion accelerating region called the "pre-sheath" over which a potential difference $U' \gtrsim \frac{1}{2} kT_e/e$ is established in order to impart a directed drift velocity to ions in the adjacent plasma; this ensures that the sheath region is fed with ions at such a rate that a balance of negative and positive charge density can be maintained in the electrostatic field close to the surface. The balance in charge density requires that the plasma drift velocity at the sheath edge is at least equal to the ion sound speed.

If ions have a Maxwellian distribution of velocities, then those which enter the sheath carry an amount of energy equal to $2kT_i$ because high energy particles preponderate over those with the average energy ($1.5 kT_i$). Positively charged ions are accelerated by the sheath potential and, if their charge state is Z , strike the surface with an energy E_i which is given by

$$E_i = 2kT_i + Ze(U + U'). \quad (3.3)$$

The repulsion of electrons by the electrostatic field reduces the density of electrons in the sheath region but each electron carries about $2kT_e$ of energy to the surface. Thus the total energy carried to the surface by each plasma ion and its associated electrons can be expressed as

$$E_{ie} = 2kT_i + Ze(U + U') + \chi_i + Z\phi_w + Z2kT_e$$

where χ_i is the ionisation threshold energy and ϕ_w is the work function of the surface. In practice the ions cannot deliver all of their energy to the surface because many of them are backscattered as energetic atoms. If the energy reflection coefficient is R_E (see Section 5) then the energy E_{ie} lost to the surface by each ion and its associated electrons is

$$E_{ie} = [2kT_i + Ze(U + U')] (1 - R_E) + \chi_i + Z\phi_w + Z2kT_e. \quad (3.4)$$

Release of impurity atoms is strongly dependent upon the energy of ions incident upon the boundary surface (see Section 5) and in this context it is advantageous to minimise the sheath potential. The potential is reduced if the plasma electrons are cooled due to inelastic atomic collisions with released impurity atoms and with recycling "hydrogen" but another mechanism is the release of secondary electrons from the surface. These electrons are accelerated by the sheath potential and enter the plasma where they can thermalise and then return to the surface. The nett loss of charge from the plasma must remain zero and so the electron current flowing through the sheath in the direction from the plasma to the surface must be greater than the accompanying flow of ion current by an amount equal to the secondary emission current. The sheath potential will therefore decrease in order to maintain this inequality (see Hobbs and Wesson⁶). However, it must be stressed that this effect is highly sensitive to the topology of the magnetic field; for example, if the field lines graze the surface then many secondary electrons are likely to be suppressed because their gyro-radius is smaller than the sheath thickness.

Plasma density ($n = n_e = n_i$) in the boundary of a typical tokamak lies in the range 10^{13} to 10^{14} cm^{-3} and the electron temperature in the range 10 to 200 eV. The Debye length is $\sim 10^{-3} \text{ cm}$ and hence the sheath region is very much smaller than the length of the plasma flow channel in the boundary because $L_{||} (a_s)$ lies in the range 0.5 to $4.0 \times 10^3 \text{ cm}$.

Particle transport in a collisional boundary plasma

Properties of plasma transport within the flow channel which feeds the sheath region are sensitive to the exchange of energy and momentum in collisions between the plasma electrons and ions.

Such exchange takes place predominantly due to multiple, small-angle Coulomb scattering collisions whose effective mean free path (for electron-electron collisions) can be expressed as

$$\lambda_{ee} = \frac{4 \times 10^{13} T_e^2}{n Z^2 \ln \Lambda} \quad [\text{cm}] \quad (3.5)$$

where $\ln \Lambda$ is the Coulomb logarithm (~ 10). The magnitude of λ_{ee} is typically a few 10^2 cm. The electron-ion collision mean free path is of comparable magnitude and in many instances plasma flow along the magnetic field from the separatrix to the edge of the plasma sheath at the limiter can be regarded as collisional. The principal aspects of such flow are shown firstly by the fluid equation for continuity,

$$\frac{d}{dz} (n v_{||} A_{||}) = S A_{||}, \quad (3.6)$$

where S is a volume source term for charged particles (ie, number of particles/unit volume/unit time), and secondly by the associated momentum equation,

$$m n v_{||} \frac{dv_{||}}{dz} = - \frac{dP}{dz} - m v_{||} S. \quad (3.7)$$

Here, $m = (m_i + m_e)$, $P = (n T_e + n T_i)$ is the plasma pressure and it is assumed that the particle source does not add momentum to the flow. Manipulation (see Morgan and Harbour⁷) yields

$$\begin{aligned} \frac{1}{v_{||}} \frac{dv_{||}}{dz} = & - \left(\frac{1}{1 - M^2} \right) \frac{1}{A_{||}} \frac{dA_{||}}{dz} \\ & + \frac{(1 + M^2)}{(1 - M^2)} \left[\frac{S}{n v_{||}} + \frac{1}{(T_e + T_i)} \frac{d}{dz} (T_e + T_i) \right] \end{aligned} \quad (3.8)$$

Here M is the Mach number of the flow and all parameters are functions of z .

The flow must start from rest at the point of symmetry which implies that $v_{||} = 0$ and $dv_{||}/dz = 0$ when $z = 0$ so that $M(0) = 0$. The flow is therefore subsonic and accelerates up to $M(\frac{1}{2}L_{||}) = 1$ at the sheath edge. In order to illustrate trends in behaviour it is useful to simplify Eq.(3.8) by the assumptions that $M^2 \ll 1$,

$dA_{||} / A_{||} = 0$ and $d(T_e + T_i)/dz = 0$. This leads to the expression

$$\frac{dv_{||}}{dz} = \frac{S}{n}, \quad (3.9)$$

which shows that the velocity gradient $dv_{||}/dz$ is directly dependent upon the local value of the particle source $S(z)$ whenever n is invariant. If such invariance of density is valid, then it is apparent that $v_{||}$ increases linearly with z where the flow channel in the boundary plasma is subjected to a uniform source of charged particles, ie $S(z) = \text{constant}$ where the channel is fed by plasma that flows across the separatrix. However, in the region close to the limiter, the channel is fed locally by ionisation of neutral particles that arise due to plasma bombardment of the limiter surface and in general $S(\frac{1}{2}L_{||}) > S(z)$. Thus there is a corresponding increase in the gradient of $v_{||}$ close to the limiter and the plasma flow accelerates until the drift velocity equals C_s at the sheath edge. Typical conditions predicted for a boundary where $S(\frac{1}{2}L_{||}) > S(z) = (\text{constant})$ are sketched in Figure 2(b).

Transport of plasma energy to the limiter

Transport of energy along a collisional flow channel to the sheath edge is dominated by the powerful effect of electron thermal conduction parallel to the magnetic field. Collisionality due to electron-electron collisions is assured because most electrons are reflected by the boundary sheaths and ultimately leave the plasma only as a consequence of electron-electron collisions. The heat flux conducted along the flow channel can be expressed as

$$-\kappa_0 T^{5/2} \frac{dT}{dz} = \frac{\alpha Q}{[A_{||}]_Q} \quad (3.10)$$

where $T = T_e = T_i$, Q is the total flow of energy in the channel assumed to be equal to the flow Q_{\perp} across the separatrix, $[A_{||}]_Q$ is the effective area of the energy transport channel and $\kappa_0 T^{5/2}$ is the thermal conductivity. The coefficient κ_0 is given by Spitzer⁸ as

$$\kappa_0 = \frac{3.15 \times 10^2}{Z_{\text{eff}} \ln \Lambda} [W(\text{eV})^{-7/2} \text{ cm}^{-1}] \quad (3.11)$$

where Z_{eff} is the effective charge state of the plasma. The parameter α is the source distribution function of the input energy and, for a uniformly distributed flow of energy into the toroidal boundary, $\alpha = z[\pi R q(r)]^{-1}$. It is apparent that the energy flux in collisional flow is strongly dependent upon T and it is unlikely that T

will appreciably exceed a few 10^2 eV even in a reactor where $\sim 10^2$ MW must be transported by conduction to the limiter. Equation (3.11) also indicates that dT/dz is small where $T \sim 100$ eV and only becomes substantial close to the limiter where inelastic collisions in the recycling plasma cause localised cooling of the plasma electrons and concomitant reduction in $\kappa_0 T^{5/2}$.

This behaviour which is also sketched in Figure 2(b) provides justification for the preceding simplification that $n(z)$ tends to invariant throughout most of the length of the flow channel. Indication of the variation in density can be obtained from manipulation of Eq. (3.8) for conditions where $T_i = T_e$ and both S and $A_{||}$ are independent of z ; this yields

$$\frac{n(o)}{n(z)} = \frac{[1 + M(z)^2]T(z)}{[1 + M(o)^2]T(o)}$$

and, since $M(\frac{1}{2}L_{||}) = 1$, so

$$n(\frac{1}{2}L_{||}) = \frac{1}{2} n(o) T(o)/T(\frac{1}{2}L_{||}). \quad (3.12)$$

The ready ability of the electrons to transport power throughout the boundary plasma implies that $[A_{||}]_Q$ can be significantly smaller than $[A_{||}]_n$ and it follows that, in collisional transport parallel to the magnetic field, the scale length for radial transport of energy, Δ_Q , will generally be smaller than Δ_n .

Convective transport

Equation (3.5) shows that λ_{ee} becomes greater than $\frac{1}{2}L_{||}$ where either n is small or T is large and in these conditions the free-streaming flow of particles and energy along the channel will not be impeded by Coulomb collisions. Even so, electrons remain the major transporters of energy due to their high mobility in the channel between the boundary sheaths. The energy flow transported by free-streaming electrons can be expressed as

$$Q_e \approx \frac{n_e}{4} A_{||} \Omega kT_e \left(\frac{8kT_e}{\pi m_e} \right)^{\frac{1}{2}}, \quad (3.13)$$

where Ω is the numerical constant (≤ 2 and dependent upon the distribution of electron velocities). Collisionless transport can become significant in the plasma that recycles close to the limiter surface because in this region the transport path tends to be less than λ_{ee} .

The sheath region is always collisionless because $\lambda_{ee} \gg \lambda_D$ and so Q_s , the energy flow through the sheath which links the channel to the limiter surface, must be by convective transport. The flow is expressed as

$$Q_s = \Gamma_s E_{ie} = n(\frac{1}{2}L_{||}) A_{||} C_s E_{ie} , \quad (3.14)$$

where Γ_s is the plasma particle flow to the limiter and E_{ie} , which is described by Eq.(3.4), is the energy deposited upon the surface by each ion and its associated electrons.

Modelling of the boundary plasma

Behaviour of the boundary plasma has been predicted by numerical codes, for example Post² and Morgan and Harbour⁷, but the physical processes involved can perhaps be identified more readily in analytical approaches, for example Harrison et al.⁹ In this latter approach the plasma conditions at the separatrix $n(o)$, $A_{||}$, and the total input energy flow $2Q_{\perp}$ over the two channels of total length $L_{||}$, are taken as input parameters that define a particular tokamak. Equations (3.14), (3.12) and (3.10) are then employed in an iterative manner to predict $n(\frac{1}{2}L_{||})$ and $T(\frac{1}{2}L_{||})$ at the sheath. The energy lost from the plasma by atomic processes, $Q_{(atomic)}$, must be assessed in a self-consistent manner so that the energy deposited by charged particle transport to the surface of the limiter can be determined from the relationship

$$Q_s = Q_{\perp} - Q_{(atomic)} . \quad (3.15)$$

To determine $Q_{(atomic)}$ it is necessary to take account of plasma surface interactions; in particular the sputtering of atoms of limiter material and also the return of plasma ions in the form of both energetic atoms and cold atoms (or molecules).

4. DIVERTORS

The wall of the toroidal vessel should be effectively shielded from direct impact of plasma particles whenever the limiter geometry, see Figure 1(b), is such that $(a_w - a_s) \gtrsim \Delta_n$. However, the flow of boundary plasma is concentrated upon the limiter surface which is liable to release impurity ions into the adjacent region of confined plasma so that the limiter acts as a source of impurities within the torus. This source can be reduced by the use of a "divertor" which is a device that deflects or "diverts" the plasma flow channel into a separate chamber appended to the containment vessel.

The concept of a divertor action is most simply appreciated in the case of a poloidal divertor. The poloidal field in a tokamak is produced by a current that is induced to flow within the plasma

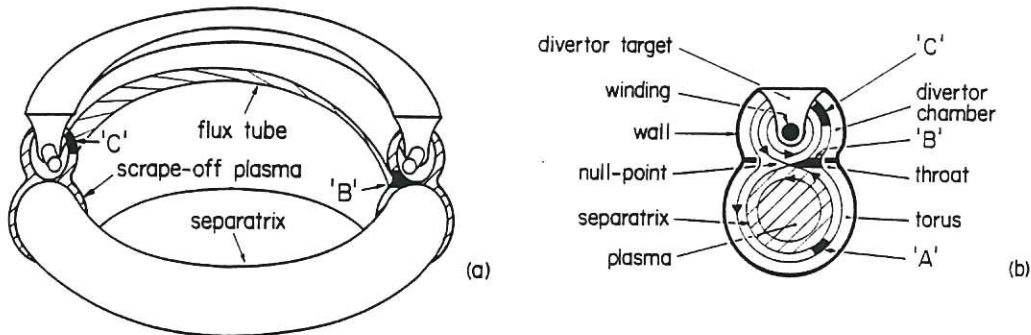


Fig.3 Schematic illustration of a tokamak with a single-null poloidal divertor.

The perspective view (a) illustrates the toroidal symmetry and the rotation of the magnetic flux tubes around the separatrix. The view in the poloidal plane (b) shows the configuration of the poloidal magnetic field and the boundary surfaces of the containment vessel together with the location of the divertor winding relative to the plasma.

and this field can be opposed (at least over a small range of poloidal angle) when a complementary current is passed in the same direction through a nearby external conductor. The poloidal divertor relies upon such local annulment and its principles are illustrated in Figure 3 where a single divertor winding is shown lying above but parallel to the magnetic axis of the plasma. Location of "the null-point" (ie, the region where $B_{pol} = 0$ in the poloidal plane) defines the separatrix and it is dependent upon the spacing between the winding and the plasma and also upon the relative magnitude of the currents. The walls of the vessel are necked-in around the null-point so that communication between the divertor chamber and the containment vessel is restricted; the system is symmetrical in the toroidal plane and additional divertor windings can be provided to increase the number of null-points. The open magnetic field lines outboard of the separatrix are twisted, in the manner shown in Figure 1(a), so that plasma at position 'A' is rotated to 'B' and then to 'C' as it moves in the toroidal direction around the torus. In effect, plasma that diffuses across the separatrix into region 'A' is scraped out of the torus and deposited upon the divertor target; indeed, the toroidal boundary plasma is termed the "scrape-off" region and the diverted field serves the role of a "magnetic limiter". The effective length of the flow channel in the scrape-off plasma is about $\pi R q(a_s)$ and the channel area $A_{||}$ is given by Eq. (2.6).

Other forms of divertor are based upon different magnetic configurations and convenient compilations of information can be found

in Harbour¹⁰ and in Ref.4.

Modelling techniques previously discussed for the plasma transport to the limiter are also applicable to the divertor, the principal difference being that neutral particles produced at the target of the divertor tend to be locally ionised and hence recycle within the divertor chamber. Thus $S(\frac{1}{2}L_{||}) \gg S(z)$ and, as a consequence, $v_{||}(z)$ within the torus is likely to be smaller than in the case of the limiter. In general, $\Delta n \sim (a_w - a_s)$ and it is predicted that divertor action will not be particularly efficient in its transport of charged particles directly from the separatrix to the divertor chamber, ie, the particle "unload efficiency" is rather low. However, the energy "unload efficiency" tends to be high because electron thermal conduction is not effected by the low drift velocity in the scrape-off region. Release of impurities by processes such as sputtering is strongly dependent upon the energy flux incident upon the boundary surfaces so that impurity atom release is concentrated at the divertor target. These impurities tend to be retained within the divertor chamber due to localised ionisation followed by entrainment of the ions in the plasma flow to the target.

5. PLASMA SURFACE INTERACTIONS

Conditions in the boundary plasma are influenced by plasma-surface interactions. The most significant are interactions associated with the return of atoms and molecules of "hydrogen" to the plasma and processes associated with the release of atomic impurities, for example, sputtering of the boundary material and desorption of impurity species. Some processes are initiated by the impact of single atoms or ions whereas others are of a macroscopic nature, eg, evaporation, unipolar arcing and flaking. A further distinction can be made between processes which involve momentum transfer (eg, ion impact) and those processes associated with irradiation of the boundary surfaces by photons and energetic electrons. A comprehensive review of the processes and data pertinent to tokamak experiments has been produced by McCracken and Stott¹¹ but, in the context of the present discussion, the scope of this broad subject area is reduced to considerations of the return of incident plasma particles and to the physical sputtering of boundary material by energetic atoms and ions.

Return of incident particles

Ions and atoms of moderate incident energy ($\sim 10^2$ eV) can pass through the surface of a solid and then be scattered by inelastic collisions within the lattice of the material. Some of the incident particles backscatter to the surface, from which they emerge with reduced kinetic energy, whereas the remainder slow down to thermal energies and are thus trapped within the lattice. Lindhard et al.¹² proposed that both the range and energy loss of the incident

particles could be characterised by a reduced energy, ϵ , given by

$$\epsilon = \frac{M_2}{(M_1 + M_2)} \frac{a}{A_1 A_2 e^2} E \quad (5.1)$$

where M_1, A_1 and M_2, A_2 are the mass and atomic numbers of the incident particle and target atom respectively and E is the incident energy. Lindhard postulated that the parameter a should be set equal to the Thomas-Fermi screening length, ie,

$$a = 0.4685 \left(A_1^{2/3} + A_2^{2/3} \right)^{-1/2},$$

so that

$$\epsilon = 32.55 \frac{M_2}{(M_1 + M_2)} \frac{1}{A_1 A_2 \left(A_1^{2/3} + A_2^{2/3} \right)^{1/2}} E(\text{keV}). \quad (5.2)$$

The probability for backscattering or "reflection" of an incident particle of energy E is described by means of a particle reflection coefficient R_N and, if E is expressed in units of ϵ , then R_N for various combinations of projectile and target has been shown to lie approximately on a universal curve. This is a function of ϵ and it

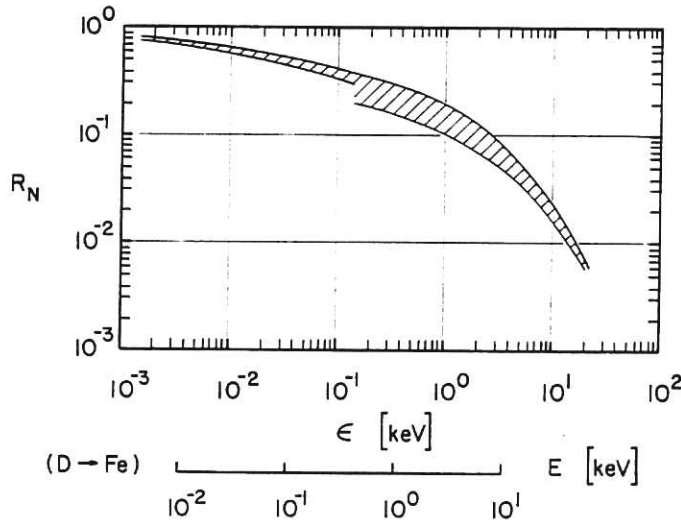


Fig.4 The reflection coefficient R_N for light atoms and ion incident normally upon surfaces plotted as a function of reduced energy ϵ .

The shaded region illustrates the spread in data presented by Eckstein and Verbeek¹³ and ϵ (in keV) is determined from Eq.(5.2). The scale of incident energy E for $D \rightarrow Fe$ is also shown.

has the form shown in Figure 4. The shaded region indicates the spread in data for light ions (biased somewhat in favour of measured values) that are taken from a compilation by Eckstein and Verbeek¹³. These data refer to particles in the energy range below 20 keV which are incident normal to the surface, but the data allow for the fact that emerging particles have an angular distribution which is close to cosine. It is apparent that ions with low incident energy are more readily backscattered than trapped and that backscattering is greatest for targets with large atomic number. The reflection coefficient is predicted to increase with deviation from normal incidence; at grazing incidence $R_N \rightarrow 1$. The reflection coefficient for incident atoms should be similar to that for ions because the charge state has little significance once the particle enters the influence of the lattice system.

The emerging particles are predominantly neutral due to electron capture within the solid; appreciably less than 1% of incident protons emerge as charged particles in the energy range of interest, ie, $E < 1$ keV.

The energy distribution of the backscattered particles is described by a coefficient R_E which is defined as the fraction of the incident energy that is reflected, ie, emerges from the surface. The coefficient R_E , expressed as a function of ϵ , also lies approximately upon a universal curve. The average energy of the backscattered atoms is R_E/R_N and this ratio is shown in Figure 5 using data taken from McCracken and Stott¹¹. The fraction of energy carried

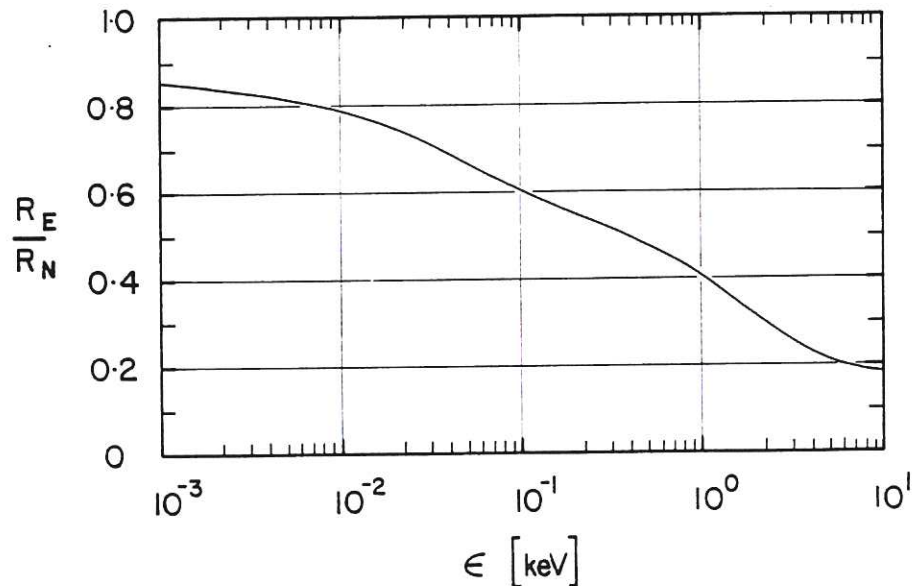


Fig.5 The average energy of reflected particles (R_E/R_N) plotted as a function of reduced energy ϵ . Data are taken from McCracken and Stott¹¹.

away by backscattered particles becomes greater as the incident energy is reduced because slow particles penetrate but weakly and so can lose little of their energy by collisions with the lattice.

Particles are trapped within the lattice system when they lose most of their initial kinetic energy but the range of penetration is small ($\sim 10^{-6}$ cm) and so the peak number density of particles within the penetration depth rapidly becomes comparable to that of the lattice atoms and the system quickly reaches equilibrium. The gradient of particle concentration is much steeper towards the surface than into the bulk material and trapped particles diffuse more readily towards the surface. In equilibrium, each incident particle is either backscattered or releases a particle that has been trapped in the solid; there is no nett retention of particles by the solid and the ratio of outgoing fluxes of backscattered to de-trapped particles is given by $R_N/(1 - R_N)$.

The de-trapping mechanisms within the lattice structure appear to be a combination of thermal release and release induced by energetic particles. The energy of the de-trapped particles is likely to approximate to the temperature of the wall and consideration of the surface binding energy favours the release of "hydrogen" in the form of molecules; this concept is frequently accepted in modelling of boundary plasma conditions.

Details of backscattering and de-trapping differ between incident ions or atoms. For normally incident particles of energy E , both species give rise to a fraction $R_N(E)$ which is backscattered with an average energy $E(R_E/R_N)_E$ and a fraction $(1 - R_N)_E$ of low energy, de-trapped particles. However, atoms tend to impact with randomly distributed incident directions and with a velocity distribution corresponding to Maxwellian. Since ions are accelerated through the sheath their energy is more closely mono-energetic and their velocity tends somewhat towards normal incidence.

Physical sputtering

Physical sputtering occurs due to the ejection of a surface atom which in some manner receives an impulse from an incident particle. Sputtering by plasma light ions has recently been reviewed by Roth¹⁴ and suffice to state here that the sputter yield has been shown to consist of two components: one due to direct transfer of momentum from the ion to an atom at the surface and the second due to backscattered projectiles that transfer momentum whilst they are exiting through the surface. The first mechanism is strongly evident at grazing incidence and gives rise to the ejection of atoms into an anisotropic cone in the forward direction. The second mechanism, which is more evident at normal incidence and higher energy, tends to display a cosine type distribution of ejected atoms. The sputter yield (atom per ion) is greatest at angles

close to grazing incidence where its value can be as high as 20 times that at normal incidence.

There is an identifiable threshold energy below which insufficient energy is transferred to the lattice atoms for sputtering to occur. This threshold, E_{th} , can be related to the sublimation energy of the solid, E_w , in the manner

$$E_{th} \approx \frac{E_w}{\zeta(1 - \zeta)} \quad (5.3)$$

where

$$\zeta = \frac{4M_1M_2}{(M_1 + M_2)^2}.$$

A recent compilation of data for sputtering by light ions at low energy (Roth et al.¹⁵) lists values of E_{th} , for example: $H \rightarrow C = 9.9$ eV; $H \rightarrow Fe = 64$ eV; $H \rightarrow Mo = 164$ eV; and $H \rightarrow W = 400$ eV. Assessment of data for low energy H^+ , D^+ , $^3He^+$ and $^4He^+$ impact upon a wide range of targets yields a universal curve for the sputtering

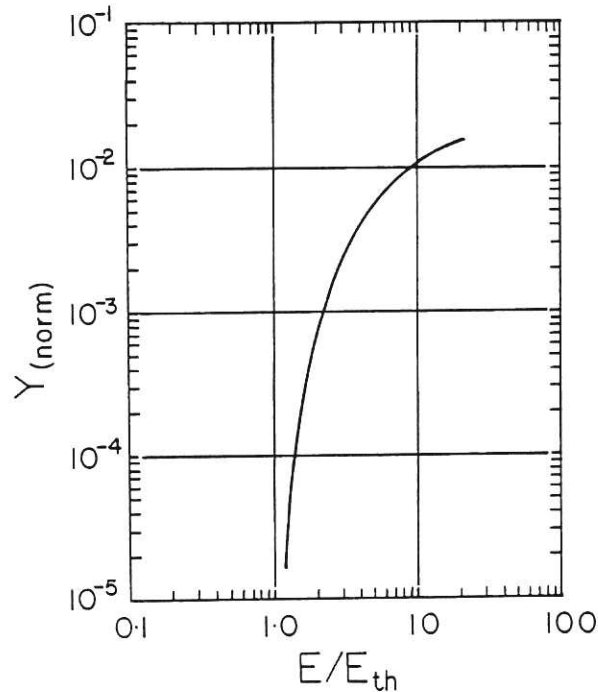


Fig.6 The normalised sputter yield $Y_{(norm)} = Y/(M_2\zeta^{5/3})$ plotted as a function of the energy parameter E/E_{th} .

Data are taken from Roth et al¹⁵ and the parameters are discussed in the text.

yield, Y , at normal angle of incidence,

$$Y = 6.4 \times 10^{-3} M_2 \zeta^{5/3} \left(\frac{E}{E_{th}} \right)^{1/4} \left(1 - \frac{E_{th}}{E} \right)^{7/2} \text{ atoms/ion.} \quad (5.4)$$

The expression describes the sputter yield to within a factor of two when $M_1/M_2 < 0.4$ and $1 < (E/E_{th}) < 20$; the dependence of the normalised yield $Y_{(norm)} = Y/(M_2 \zeta^{5/3})$ upon E/E_{th} is shown in Figure 6.

The magnitude of Y is illustrated in Figure 7 for various ions incident upon a nickel target. Curves through the data points show the fit of the energy dependence of Eq.(5.4). It is apparent that the sputter yields for "hydrogen" ions are not substantial in the energy range appropriate to the boundary plasma but the corresponding yield for self-sputter of Ni by Ni can exceed unity. Effects of self-sputtering can be significant because the initially sputtered atom becomes ionised by collisions with the plasma electrons and returns to the surface upon which it impacts with the energy gained due to acceleration through the plasma sheath, see Eq.(3.3). During this recycling period it is likely that the ion will suffer several ionising collisions with electrons which raise its charge state to a moderately high level (see Section 6); self-sputtering therefore becomes significant even at modest electron temperatures, eg, T_e ranging from 20 to 60 eV. This recycling of sputtered material introduces radiating impurity ions into the boundary regions which in

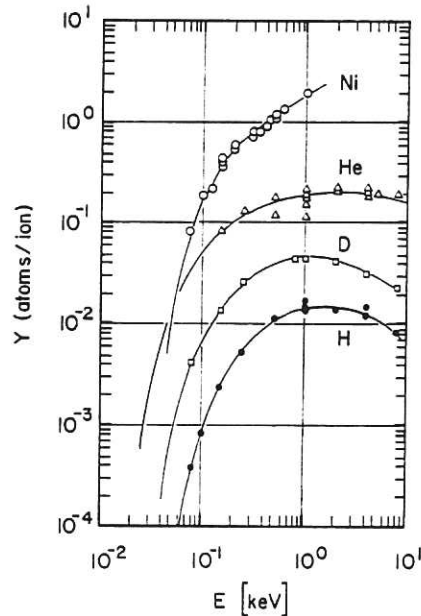


Fig.7 The sputtering yield Y plotted as a function of energy E for ions at normal incidence upon nickel.

Data are taken from Roth et al.¹⁵

turn cause localised cooling of the plasma electrons and a concomitant reduction of the sheath potential and hence the sputter yield. The system may be self-regulating in the sense that the sputtering rate becomes stabilised when power carried to the localised region of impurities by electrons in the plasma is balanced by power radiated from the impurities. The consequences of this action are considered in Section 7.

6. ATOMIC PROCESSES IN THE BOUNDARY PLASMA

Significant effects of atomic reactions in the boundary region relate predominantly to free-bound collisions and the most prolific bound species is "hydrogen" (either atomic or molecular). There are also smaller concentrations of impurity atoms and ions. Low mass impurities such as oxygen and carbon arise from de-trapping of surface gases or from sputtering of carbon surfaces, medium mass elements such as iron are produced by erosion of the containment vessel which is frequently constructed from stainless steel whereas tungsten (or other high mass refractory elements) may be present due to erosion of limiters or divertor targets. In a DT burning reactor there will also be helium. These atoms enter the plasma with an initial velocity that is governed by surface interactions and their subsequent collision rate with charged plasma particles can be expressed as

$$K = n n_0 \langle \sigma \bar{v} \rangle . \quad (6.1)$$

Here n and n_0 are respectively the density of the plasma and the neutral species, \bar{v} is their relative velocity, σ is the cross section for the process and $\langle \sigma \bar{v} \rangle$ is averaged over the Maxwellian velocity distribution of the collisions. In general, collisions with electrons are the most frequent because of the comparatively high electron velocity but some heavy particle collisions, such as symmetric, resonant charge exchange



can also be significant because of the large magnitude of the cross section at low collision energy. Charge exchange between impurity ions and high velocity "hydrogen" atoms can result in appreciable deposition of power in the boundary during neutral beam heating.

The plasma can be regarded as transparent to most radiation emitted by free-bound transitions and so photon induced reactions can be neglected. Inelastic atomic collisions involving electrons remove thermal energy from the electron component of the plasma by exciting radiative transitions in "hydrogen" atoms and in atoms and unstripped ions of impurities. Electron energy is also dissipated in ionising collisions. Electron-ion recombination in the boundary is unlikely, firstly because the electron density is insufficient

to support three body recombination and secondly because the characteristic time, τ_α , for two body radiative recombination,

$$\tau_\alpha = [n_e \alpha(T_e)]^{-1}, \quad (6.2)$$

is too great for recombination to occur at a significant rate. The two body recombination rate coefficient $\alpha(T_e)$ of unstripped ions is relatively large due to the contributions from dielectronic recombination for which $\tau_\alpha > 10^{-2}$ s. This is several orders less than τ_α for electron-"proton" two body radiative recombination but, since the unstripped impurity ions tend to be concentrated close to the boundary surfaces, the ion residence time, τ_{imp} , must be appreciably less than the residence time of the bulk of the boundary plasma for which $\tau_{||} \sim 10^{-3}$ s (see Section 2). Thus, τ_{imp} is appreciably less than τ_α and two body recombination can be neglected.

Dissipation of electron energy due to collisions of electrons with "hydrogen" atoms

The most significant atomic processes associated with electron collisions with "hydrogen" atoms are:

- a. Excitation of an atom from level (p) to an upper level (q),



which may be followed by spontaneous radiative decay,



- and b. Ionisation of an atom in level (p),



An important associated reaction is collisional de-excitation which is the reverse of (ii) and this is a super-elastic process which returns energy to the colliding electron.

The implications of these electron impact processes are discussed in detail in papers by Bates et al.¹⁶, Bates and Kingston,¹⁷ McWhirter and Hearn¹⁸ and Hutcheon and McWhirter¹⁹. It is postulated that electron collisions cause ionisation either directly, by transferring a bound electron to the continuum, or indirectly through a sequence of level transitions which terminates in the continuum. The cross sections for such level transitions are large, proportional to n^4 where n is the principal quantum number, and so

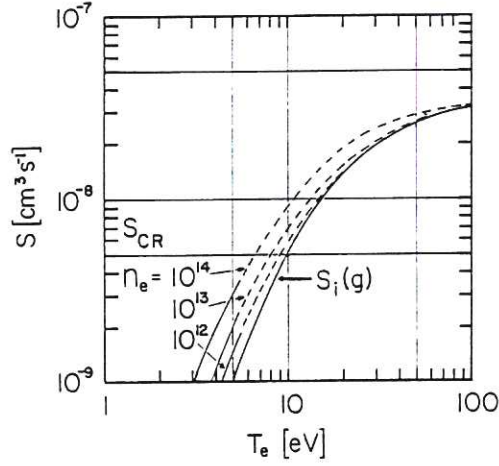


Fig.8 The rate coefficient for electron impact ionisation of hydrogen atoms. The collisional-radiative ionisation coefficients S_{CR} are taken from Bates et al¹⁶ and shown for electron densities of 10^{12} , 10^{13} and 10^{14} cm^{-3} . $S_i(g)$ is the ground state ionisation coefficient corresponding to conditions of low electron density.

the collision time,

$$\tau_n = (n_e \langle \sigma_n v_e \rangle)^{-1}, \quad (6.3)$$

becomes shorter than the radiative lifetimes of all but the lowest lying excited states; the lifetime of high n states is proportional to n^3 . The probability of spontaneous emission is thereby reduced in favour of (a) ionisation by a chain of non-radiative upward transitions and (b) repopulation of the ground state by a complementary chain of non-radiative downward transitions. Within the boundary plasma τ_n is appreciably less than the particle residence time so that the probability of ionisation is enhanced by non-radiative transitions and the ionisation rate can be expressed as

$$K_i = n_e n(g) S_{CR}. \quad (6.4)$$

Here $n(g)$ is the density of ground state species and S_{CR} is a composite coefficient, called the "collisional radiative ionisation coefficient," which allows for the processes outlined above. S_{CR} is compared with the ground state coefficient $S_i(g)$ in Figure 8.

The preceding discussion leads to the concept that electrons colliding with a partially ionised "hydrogen" plasma lose energy by ionisation and by radiation from a few low lying radiative levels and the average amount of energy, ξ_i , expended in producing one proton-electron pair must include contributions from both processes.

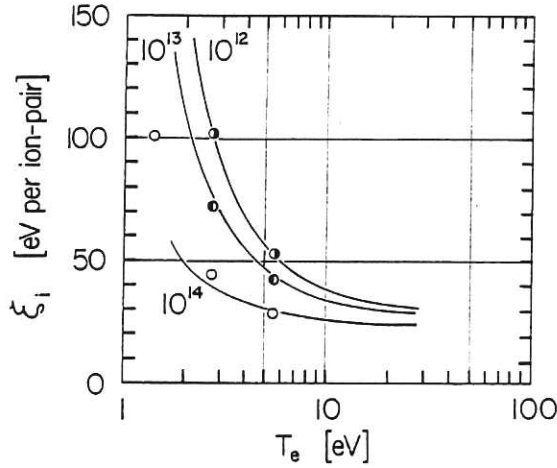


Fig.9 The average electron energy ξ_i dissipated in producing one proton-electron pair in atomic hydrogen plotted as a function of electron temperature T_e . Solid lines show the data of McWhirter and Hearn¹⁸ for hydrogenic ions. Data for H atoms (taken from Bates et al¹⁶ and Bates and Kingston¹⁷) are shown by circles.

McWhirter and Hearn¹⁸ have evaluated ξ_i for hydrogen-like ions in conditions where recombination is insignificant; the appropriate expression is

$$\xi_i = \frac{(\chi_i S_{CR} + P_1 n_e^{-1})}{S_{CR}}, \quad (6.5)$$

where $P_1(T_e, n_e)$ is a coefficient that allows for radiative power loss from ground state ions. The data appropriate to $Z = 1$ (ie, equivalent to "hydrogen") are shown as a function of T_e (for $n_e = 10^{12}, 10^{13}$ and 10^{14} cm^{-3}) by the solid lines in Figure 9. The parameters scale for fully stripped ions with $Z > 1$ according to

$$[T_e]_Z \equiv Z^2 T_e; [\xi_i]_Z \equiv Z^2 [\xi_i]_H \text{ and } [n_e]_Z \equiv n_e Z^{-7} \quad (6.6)$$

and, because of the strong sensitivity of $[n_e]_Z$ upon Z , it is unlikely that non-radiative processes will influence the ionisation rates of fully stripped impurity ions.

This analysis is directed towards electron hydrogenic-ion collisions and so employs Coulomb-Born cross sections which over-estimate excitation and ionisation in electron-atom collisions except at high T_e . To show the significance of this effect data for H atoms (S_{CR} from Bates et al.¹⁶ and P_1 from Bates and Kingston¹⁷) have been substituted into Eq.(6.5) and the results plotted as circles in Figure 9.

It is also worth noting that each ionising event involved in the recycling of "hydrogen" atoms corresponds to an amount of energy ($\xi_i - \chi_i$) extracted from the plasma electrons and subsequently radiated to the wall, whereas χ_i is transferred from the electrons and stored as potential (not kinetic) energy in the plasma ions. The initial energy of the ions corresponds to that of their parent atoms whereas most of the secondary electrons are emitted with low energy (a few eV being typical). Subsequent Coulomb collisions with the bulk plasma tend to bring the energies of the ions and secondary electrons into equilibrium with the plasma temperature. The time, t_T , required for a test particle of temperature T' to reach the temperature T of the plasma has been given by Spitzer⁸ as

$$t_T = \frac{7.34 \times 10^6 M'M}{n Z'^2 Z^2 \ln \Lambda} \left(\frac{T'}{M'} + \frac{T}{M} \right)^{3/2} \quad [s] \quad (6.7)$$

and so the temperature attained by the recycling ions and electrons is governed by the ratio of their residence times to the appropriate value of t_T .

The influence of charge exchange and the recycling of 'H' atoms

The rate coefficients for charge exchange and electron impact ionisation are such that, in a homogeneous plasma, the frequency of charge exchange collisions is greater than that of ionising collisions. During each charge exchange collision a plasma proton captures an electron and the resultant atom moves freely across the magnetic field in a direction which is almost randomly distributed around the collision site. In effect, the collision scatters the plasma "proton" so that it moves (as an atom with energy corresponding to the ion temperature) either outward towards the wall or inward towards the region of hotter plasma. A sequence of such charge exchange collisions may take place before the transported atom is ionised and at each collision the resultant atom has the local temperature of the plasma "protons." Molecules of "hydrogen" do not play a direct role in this cycle because their cross-section for charge exchange is relatively small; nevertheless, they are readily dissociated in collisions with electrons and their product atoms subsequently undergo charge exchange. These atomic processes govern the distribution of energy amongst those "hydrogen" atoms that return to the wall.

Transport of atoms can be assessed using Monte Carlo techniques which take account of the changes in both direction and energy that result from collisions of atoms with both plasma ions and boundary surfaces; see, for example, Heifetz et al.²⁰ Alternative approaches, eg, Harrison et al.⁹ are based upon analytical methods that describe a random walk but the significance of atomic processes can be illustrated by using a simplified version,

Harrison³, that assesses the probability that an atom released from the wall will recycle back to the wall as a "daughter" atom.

Consider two conditions, an initial one (a), where an atom has a velocity v_0 characteristic of its release from boundary surface and a subsequent one (b), where the velocity has been changed by collision with a plasma proton so that the "daughter" atom corresponds to a randomly directed particle with thermal velocity v_{th} . The plasma is assumed to be homogeneous and of infinite extent and motion is considered only in the direction x normal to the surface. The flux Γ^a of condition (a) atoms at a distance x is given by

$$\Gamma^a(x) = \Gamma^a(0) \exp^{-\frac{x}{\Delta_a}}$$

where

$$\frac{1}{\Delta} = \frac{1}{\lambda_{cx}^a} + \frac{1}{\lambda_i^a} \quad (6.8)$$

and λ_{cx}^a and λ_i^a are respectively the mean free path for charge exchange and electron ionisation. In an element of extent dx at x , there is a rate,

$$K^a(x) \approx \Gamma^a(x) \frac{dx}{\lambda_{cx}^a},$$

of charge exchange collisions which produce condition (b) daughter atoms that move with equal probability either more deeply into the plasma (where they are assumed to be trapped by ionisation) or else backwards towards the surface. Motion in condition (b) can be treated as a diffusive problem in which the diffusion step length corresponds to the charge exchange mean free path λ_{cx}^b . Diffusion need be considered only in one direction and so the scale length, Δ_b , of diffusive transport can be expressed as

$$\Delta_b \approx \left(\frac{N_b}{3}\right) \lambda_{cx}^b. \quad (6.9)$$

Here N_b is the average number of charge exchange collisions prior to ionisation and it is equal to the ratio of collision times, namely,

$$N_b \approx \frac{\tau_i^b}{\tau_{cx}^b} \approx \frac{\lambda_i^b}{\lambda_{cx}^b} \approx \frac{1}{G_b}$$

where G_b is the ratio of the electron ionisation to the charge exchange rate coefficients, ie, $G_b = S_{CR}^b / S_{cx}^b$. The atoms returning from dx at x are in condition (b) and their flux at the wall, $\Gamma^b(x)$, is given by

$$\Gamma^b(x) \approx \frac{1}{2} K^a(x) \exp^{-\frac{x}{\Delta_b}}.$$

Manipulation and integration yields the probability Γ^b/Γ^a that a daughter atom returns to the wall, namely,

$$\frac{\Gamma^b}{\Gamma^a} \approx \frac{1}{2} \frac{1}{\lambda_{cx}^a} \cdot \frac{\Delta_a \Delta_b}{(\Delta_a + \Delta_b)}, \quad (6.10)$$

which can be expressed as

$$\frac{\Gamma^b}{\Gamma^a} \approx \frac{1}{2} \left[1 + G_a + (3G_b)^{\frac{1}{2}} \frac{\lambda_{cx}^a}{\lambda_{cx}^b} \right], \quad (6.11)$$

where G_a is the ratio of rate coefficients for condition (a) atoms.

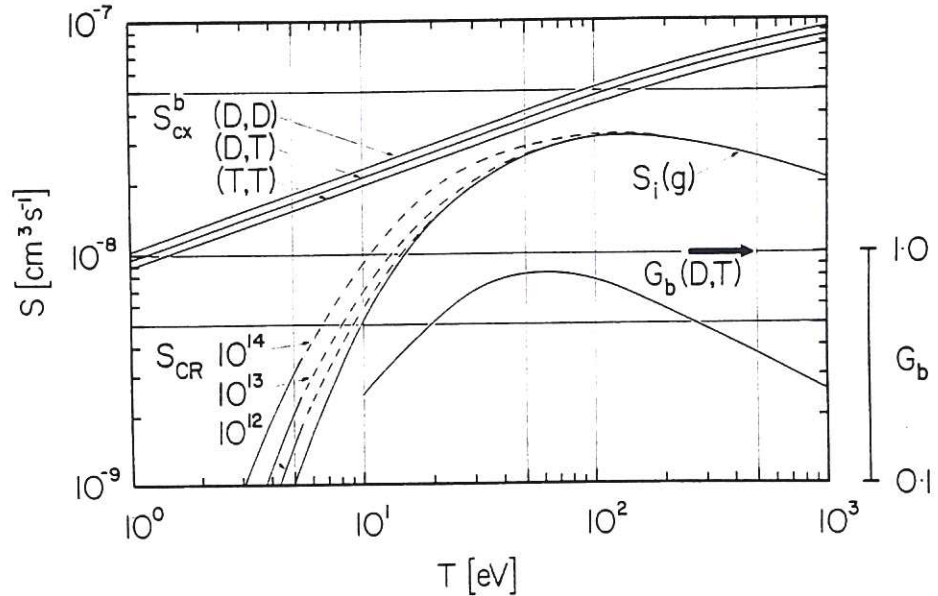


Fig.10 Rate coefficients for charge exchange and electron impact ionisation plotted as a function of plasma temperature T .

The analytical form of the charge exchange cross section is taken from Riviere²¹ and the influence of isotope mass is shown by S_{cx}^b plotted for DD, TT and DT. The ratio $G_b = S_{CR}^b / S_{cx}^b$ is shown for D→T collisions.

The charge exchange mean free paths are given by

$$\lambda_{cx}^a = \frac{v_o}{n_i \langle \sigma_{cx} \bar{v}_{op} \rangle} \quad \text{and} \quad \lambda_{cx}^b = \frac{v_{th}}{n_i \langle \sigma_{cx} \bar{v}_b \rangle},$$

where \bar{v}_{op} is the relative velocity of a collision involving an atom with velocity v_o and a plasma "proton" with thermal velocity v_{th} . For condition (b) collisions, \bar{v}_b is given by

$$\bar{v}_b = \left[\frac{8kT_i}{\pi} \frac{(m_o + m_i)}{m_o m_i} \right]^{\frac{1}{2}},$$

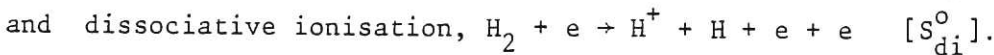
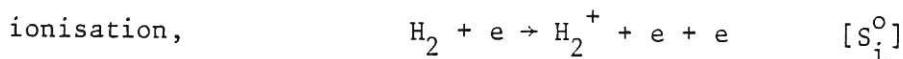
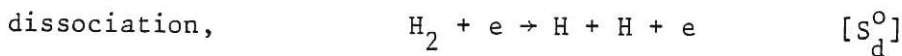
where m_o and m_i are respectively the masses of the atom and plasma ion.

Sensitivity of H atom recycling to atomic processes can be identified from Figure 10 where S_{cx}^b , S_{CR} and G_b are shown as functions of plasma temperature $T = T_e = T_i$. The ratio G for both conditions (a) and (b) is rather insensitive to T over the range 20 to 200 eV which typifies many boundary regimes. The preceding simple assessment indicates that a typical value of the probability of Γ^b/Γ^a appropriate to fast backscattered atoms (ie, $v \rightarrow v_{th}$) is about 0.17 but this probability increases as the atom release velocity is reduced to a limiting value of about 0.3 when $v_o \rightarrow 0$.

Effects of molecular "hydrogen"

Inelastic collisions of electrons with neutral molecules of "hydrogen" extract thermal energy from the electron component of the plasma in a manner comparable to electron "hydrogen" atom collisions. There is a lack of data pertinent to the radiative power losses associated with the production of an (electron + H_2^+) ion-pair and so the difference between H_2 and H is not usually distinguished when determining radiative power losses. However, it is important to assess the degree of molecular dissociation in order to account for the component of "H" atom recycling that arises as a consequence of the presence of "hydrogen" molecules.

The most significant collisions between electrons and neutral "hydrogen" molecules are:



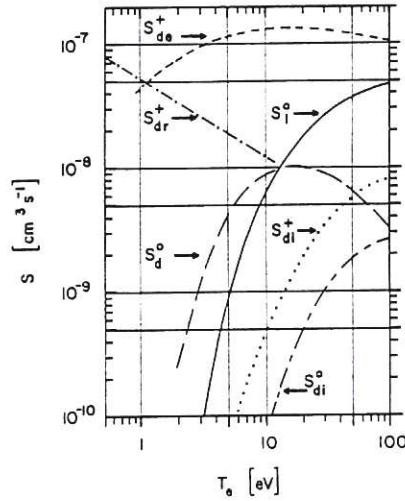


Fig.11 Rate coefficients for electron collisions in H_2 and H_2^+ plotted as a function of electron temperature T_e . Rate coefficients for neutral molecules, S^0 , are taken from Jones²² and those for ions, S^+ , are discussed by Harrison.³ The subscripts identify the reactions discussed in the text.

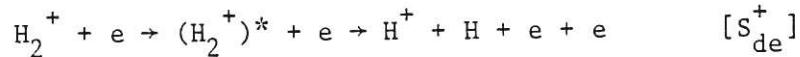
Experimental data for these reactions are available and the rate coefficients, S_d^0 , etc, calculated by Jones²² are plotted in Figure 11. It is evident that dissociation into two H atoms predominates at low electron temperature whereas formation of H_2^+ is the most significant reaction where $T_e \gtrsim 10$ eV. These data refer to molecules in their ground vibrational state and they can be employed in plasma modelling with the reservation that some of the detrapped molecules may be vibrationally excited.

The most significant collisions involving H_2^+ are:

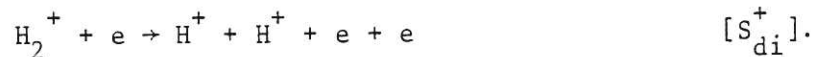
dissociative recombination,



dissociative excitation,



and dissociative ionisation,



Experimental data for H_2^+ have been reviewed by Dolder and Peart²³ and the status of the corresponding rate coefficients has been discussed by Harrison.³ The appropriate rate coefficients for the molecular ion, S_{dr}^+ , etc, are plotted in Figure 11 and refer to ions

which have a distribution of vibrationally excited levels that is closely determined by the appropriate Frank-Condon factors (see for example, Dunn²⁴). Dissociative excitation of H_2^+ into H^+ and H is the most powerful process when $T_e \gtrsim 5$ eV and so any H_2^+ formed from neutral H_2 molecules will almost immediately dissociate. Dissociative recombination into H atoms is the dominant process for the destruction of H_2^+ at low T_e but relatively few H_2^+ ions can be formed at such low temperatures.

It is reasonable to express the rate coefficient $S^0(H^+)$ for the formation of protons from H_2 neutral molecules as

$$S_2^0(H^+) \approx S_i^0 \left(\frac{S_{de}^+ + 2S_{di}^+}{S_{de}^+ + S_{di}^+} \right) + S_{di}^0 \quad (6.12)$$

and that for the formation of H atoms as

$$S_2^0(H) \approx 2S_d^0 + S_{di}^0 + S_i^0 \left(\frac{S_{de}^+}{S_{de}^+ + S_{di}^+} \right). \quad (6.13)$$

Thermal energy neutral "hydrogen" molecules that are formed by detrapping of "hydrogen" from boundary surfaces will penetrate but weakly into the plasma because of their low velocities. The charged dissociation products are trapped by the magnetic field and become entrained in the plasma flow that drifts to the surface. The neutral "H" atom products can penetrate more deeply into the plasma.

The effects of electron collisions with impurity elements

Electrons dissipate energy by exciting radiative transitions in atoms and unstripped ions of the impurity components of the plasma. Moreover, the charge state reached by the impurity atoms before they return to the boundary surface has a powerful effect upon the rate of surface erosion (see Section 5). Impurity ions within the boundary plasma will not be in local-thermal-equilibrium with plasma electrons because the ion residence time, $\tau_{||}^+$, is shorter than the electron-ion recombination time τ_α and the coronal equilibrium conditions for charge state populations will not apply, ie,

$$\frac{n_Z}{n(Z-1)} \neq \frac{S_{i,(Z-1)}(T_e)}{\alpha_Z(T_e)}. \quad (6.14)$$

To account for this situation Shimada et al.²⁵ and Abramov²⁶ introduce an ion loss term into the rate equations for charge balance,

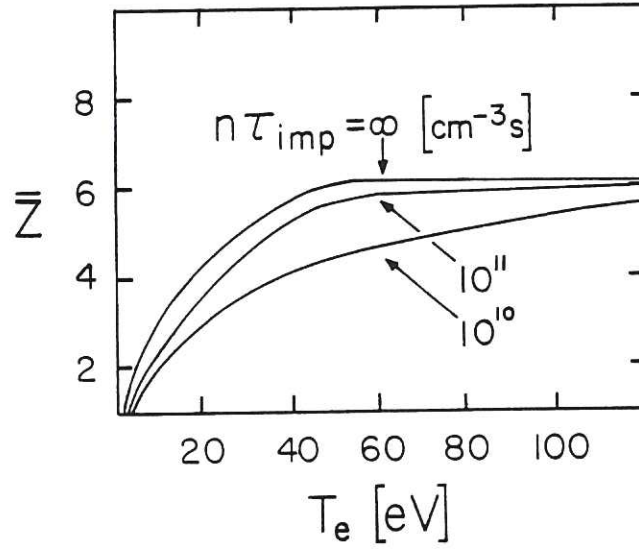


Fig.12 The average charge state \bar{Z} of oxygen ions plotted as a function of electron temperature T_e . Data for $\bar{Z} = \sum n_Z Z / \sum n_Z$ are taken from Abramov²⁶ and are shown for several values of the product $n\tau_{\text{imp}}$ where the ion residence time τ_{imp} is independent of Z . Conditions when $n\tau_{\text{imp}} \rightarrow \infty$ correspond to coronal equilibrium.

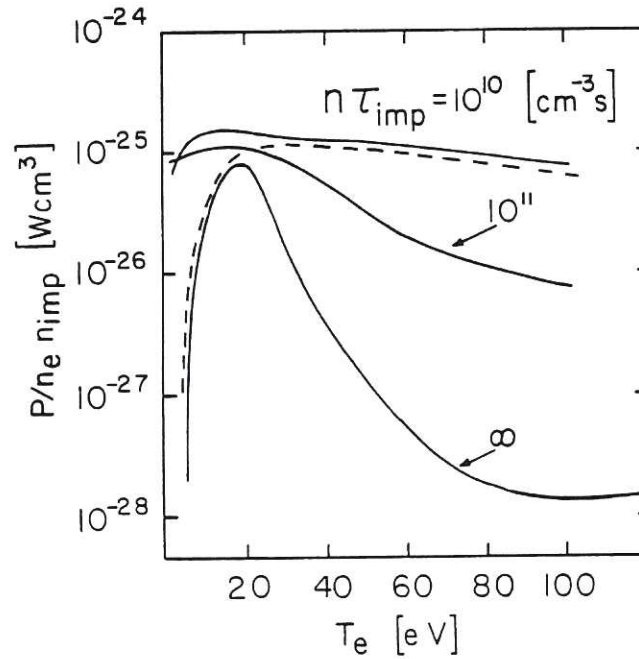


Fig.13 The radiated power function $P/n_e n_{\text{imp}}$ for oxygen plotted versus the electron temperature T_e . Data of Abramov²⁶ are shown by the solid lines, those of Shimada et al²⁵ by the dashed line.

eg,

$$n_e n_{(Z-1)} S_{i,(Z-1)} - n_e n_Z S_Z + n_e n_{(Z+1)} \alpha_{(Z+1)} - n_e n_Z \alpha_Z - n_Z \tau_{imp}^{-1} = 0. \quad (6.15)$$

The temperature dependence of the average charge state of oxygen determined by Abramov²⁶ for $n\tau_{imp}$ values of 10^{10} and $10^{11} \text{ cm}^{-3} \text{ s}$ is shown in Figure 12; the average charge state is lower than predicted by the coronal equilibrium model. The radiated power function, ie, $P(n_e n_{imp})^{-1}$ where $n_{imp} = \sum n_Z$, is shown in Figure 13 and it is apparent that these non-coronal models predict substantially greater power losses due to radiation when $T_e > 30 \text{ eV}$.

An alternative approach, Harrison,³ is based upon the determination of the characteristic loss of energy associated with each stage of ionisation experienced by the impurity particle during its residence time, τ_{imp} , within the plasma. Electron-ion recombination is neglected and it is assumed that ionisation proceeds in a step-wise manner in which ΔZ is unity. The total amount of energy associated with the ionisation cycle of each released impurity atom can then be expressed as

$$\begin{aligned} \xi_{imp} = & P_{01} (\xi_o^r + \chi_o) + P_{01} P_{12} (\xi_1^r + \chi_1) \\ & + P_{01} P_{12} P_{23} (\xi_2^r + \chi_2) + \dots \quad [\text{eV/atom}] \end{aligned} \quad (6.16)$$

where ξ_Z^r is the radiative loss associated with each ionisation step and the upper limit of charge state is determined by the residence time or by the fully stripped condition of the ion. The parameters P_{01}, P_{12} , etc, denote the probability that the impurity atom passes through that particular stage of ionisation during its time within the plasma and it is implicit that $P_{01} = 1$. If the residence time, τ_{imp} , is known, then the probabilities can be determined from

$$P_{Z \rightarrow (Z+1)} = 1 - \exp\left(-\frac{\tau_{imp}}{\tau_{i,Z}}\right), \quad (6.17)$$

where

$$\tau_{i,Z} = (n_e S_{i,Z})^{-1}$$

is the characteristic time for ionisation.

The energy, ξ_Z , extracted from the plasma electrons during each

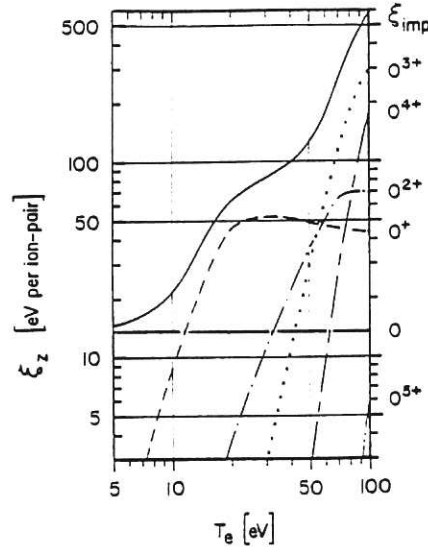


Fig.14 Electron energy dissipated by recycling oxygen ions.

Data are taken from Harrison³ and refer to oxygen atoms whose initial energy is very much less than T_e . Atomic data are taken from Summers and McWhirter.²⁷

stage of ionisation can be determined from

$$\xi_Z = \chi_Z + \left(\frac{P_{LZ}(n_e, T_e)}{S_{C\alpha}(n_e, T_e)} \right)_Z \quad (6.18)$$

where P_{LZ} is a "line radiated power loss coefficient" and $S_{C\alpha}$ is the "collisional dielectronic ionisation coefficient" which is analogous to S_{CR} used previously for ionisation of hydrogenic ions.

The residence time τ_{imp} is dependent upon the entrainment of impurity ions within the flowing boundary plasma and also upon the topology of the magnetic field and boundary surfaces (a brief description can be found in Harrison et al.⁹) but, to indicate the power loss, the data for ξ_Z presented in Figure 14 has been determined using the assumption that the impurity atoms are emitted with a temperature $T' \ll T$ and that $[\tau_{imp}]_Z \approx [\tau_T]_Z$ where $[\tau_T]_Z$ is the thermal equilibration time given by Eq.(6.7). Contributions from each charge state up to $Z = 5$ are shown and it is apparent that the effects of charge states greater than $Z = 3$ are not likely to be significant in conditions when $T_e \lesssim 50$ eV.

The preceding data take no account of the fate of secondary electrons produced by ionisation. These will be heated by electron-electron collisions and the cooling effect upon the plasma can be substantial if the ions become highly charged. For example, an ionisation cycle that extends to $Z = 4$ in a plasma where $T_e = 100$ eV

is likely to introduce an additional energy loss of 600 eV per emitted atom.

7. INTERACTION BETWEEN THE BOUNDARY AND THE CONFINED PLASMA

The preceding discussions have treated the boundary plasma in isolation from the confined plasma inboard of the separatrix. In reality these regions are closely coupled, the boundary acting as a sink for energy transported outward across the separatrix and as a neutralising region for the outward flow of plasma ions. However, "hydrogen" atoms may recycle between the two regions and the energetic daughter atoms from the hot central plasma can cause serious erosion of the torus wall. There is also an inward flow of ions from the boundary due to cross field diffusion of the boundary plasma as it drifts to the limiter or divertor. This latter aspect is particularly significant in the case of impurity ions which may diffuse inboard of the separatrix and radiate energy from the central plasma. The acceptable concentration of impurity ions within the central plasma is dependent upon the balance between the power input to the plasma, eg, the power deposited by α -particle heating within a burning DT reactor, and the power lost to the walls by atomic radiation. As a guideline, the concentration of low mass elements, eg, beryllium, carbon, etc, may be about 10^{-2} but high mass elements, eg, tungsten, should not exceed 10^{-4} .

Inward transport of impurities due to plasma-surface processes can be reduced by using a divertor although the effect is likely to be less powerful for impurities released by atom recycling to the torus wall because, subsequent to ionisation within the boundary, these particles take some time to drift into the protective environment of the divertor chamber. A limiter does not provide the advantageous segregation of the plasma bombarded surface from the separatrix and it is therefore more likely to cause impurity contamination. However, it may be possible to reduce this effect by operating the boundary plasma in conditions of high density and low temperature. At low temperature, bombardment by both ions and atoms is unlikely to cause substantial sputtering and, if the density is high, the torus walls are shielded from the direct impact of those energetic daughter atoms which move outward from the central plasma. To attain these conditions it is necessary to cool the edge plasma (ie, the boundary and possibly the inboard region adjacent to the separatrix) and this cooling can be performed by radiating impurity ions. However, it is essential that the radiative losses occur predominantly in the edge plasma and that excessive accumulation of impurity ions does not occur in the very hot core of the central plasma. If the limiter surface is formed from a medium or high mass metal, then the electron temperature of the boundary plasma may be self-regulated by the effects of self-sputtering discussed in Section 5.

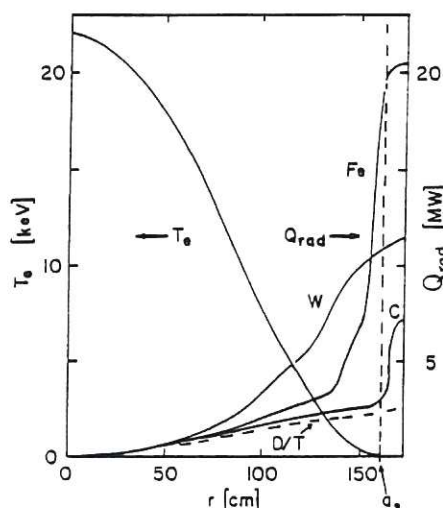


Fig.15 Radial characteristics of the radiated power loss Q_{rad} and the electron temperature T_e predicted for a limiter bounded plasma in JET. Data for limiters made from either carbon, iron or tungsten are taken from Neuhauser et al³⁰; the heating power is 28 MW.

Radiatively cooled plasma edge

The preceding concept of a limiter in a radiatively cooled plasma edge has been proposed as a suitable operational mode for the JET experiment, see Gibson,²⁸ and the scheme has been named the "cool plasma mantle." To predict plasma performance it is necessary to link the radial properties of plasma transport across the magnetic field to the physical processes discussed here in respect to transport along the field to the boundary surfaces. To date this has not been achieved using a fully self-consistent description of the boundary region but simplified versions of the boundary have been linked to one-dimensional radial transport codes, eg, Watkins et al.²⁹ Another example from Neuhauser et al.³⁰ is illustrated in Figure 15 for conditions where the limiters are constructed of either carbon, iron or tungsten. The noteworthy features of this prediction are that significant radiation losses from carbon occur only within the boundary plasma, iron radiates only within the edge plasma whereas a substantial fraction of tungsten radiation emanates from the hotter plasma core. It is particularly interesting to note that the powerful atomic radiating ability of tungsten is compensated by the lower sputter yield so that the concentration of tungsten is low and the total radiation losses are less than those from iron impurity ions.

8. CONCLUSION

It is apparent that the boundary behaviour has substantial

impact upon the performance of a magnetic confinement fusion device. Aspects such as the adoption of a divertor as a limiter have bearing upon the capital cost of a reactor and these considerations are at present critical issues in the forward planning of fusion research. An appreciation of the problems calls for a self-consistent interrelation of plasma transport, surface interactions and atomic processes. These must also be linked to the constructional and maintenance requirements of the containment vessel; such aspects as thermal and electromagnetic stresses must be taken into account and consideration given to the exposure of the system to neutron bombardment.

Another important aspect is the need to exhaust neutral helium atoms from a DT burning reactor. Studies of this requirement are based upon prediction of the neutral particle fluxes to the wall of containment vessel coupled to assessment of the ability of the vacuum pumps to extract the helium component; examples of such studies are Heifetz²⁰ and Harrison et al.⁹.

Consideration of the boundary plasma as an integral subject for study is a relatively new concept but it has now become an area of considerable activity and it is one which offers stimulating problems for the future.

REFERENCES

1. International Tokamak Reactor: Phase One, IAEA Vienna (1982).
2. D. E. Post, D. Heifetz and M. Petravic, in: "Proc. 5th Conf. on Plasma Surface Interactions in Controlled Fusion Devices", Gatlinburg, May 1982 (to appear in J.Nucl.Mater.)
3. M. F. A. Harrison (1982) in: "Applied Atomic Collision Physics" ed. H. S. W. Massey, B. Bederson and E. W. McDaniel (Academic Press) Vol.2.
4. IAEA Technical Committee Meeting on Divertors and Impurity Control (ed. M. Keilhacker and U. Daybelge, Max-Planck-Institut für Plasmaphysik, Garching, 1981).
5. F. F. Chen (1974) "Introduction to Plasma Physics", Plenum Press, New York.
6. G. Hobbs and J. Wesson (1967), Plasma Physics 9, 85.
7. J. G. Morgan and P. J. Harbour (1980) in: "Fusion Technology" (Proc. 11th Symp., Oxford) Vol.2, Pergamon, p.1187.
8. L. Spitzer (1962), "Physics of Fully Ionised Gases", John Wiley and Sons Inc., New York.
9. M. F. A. Harrison, P. J. Harbour and E. S. Hotston (1981b), in: "European Contributions to the Conceptual Design of the INTOR Phase 1 Workshop", Euratom, EURFUBRU/XII-132/82/EDV2, Brussels, 1982) 231. (To appear in Nuclear Technology/Fusion.)
10. P. J. Harbour (1981) in: "Plasma Physics for Thermonuclear Fusion Reactors" (ed. G. Casini) Harwood Academic Publishers, Paris (for the Commission of the European Communities) 255.

11. G. M. McCracken and P. E. Stott (1979), Nucl.Fusion 19, 889.
12. L. Lindhard, M. Sharff and H. E. Schiøtt (1963), Mat.Fys.Medd. 33, 39.
13. W. Eckstein and H. Verbeek (1979), Max-Planck-Institut für Plasmaphysik, Report IPP9/32.
14. J. Roth (1980), "Proceedings of the Symposium on Sputtering" Vienna 1980.
15. J. Roth, J. Bohdansky and W. Ottenberger (1979), Max-Planck-Institut für Plasmaphysik, Report IPP9/26.
16. D. R. Bates, A. E. Kingston and R. W. P. McWhirter (1962), Proc.Roy.Soc. A267, 297.
17. D. R. Bates and A. E. Kingston (1963), Planet and Space Science 11, 1.
18. R. W. P. McWhirter and A. G. Hearn (1963), Proc.Phys.Soc. 82, 641.
19. R. J. Hutcheon and R. W. P. McWhirter (1973), J.Phys.B. 6, 2668.
20. D. Heifetz, D. Post, M. Ulrickson and J. Schmidt, in: "Proc. 5th Conf. on Plasma Surface Interactions in Controlled Fusion Devices" Gatlinburg, May 1982 (to appear in J.Nucl.Mater.)
21. A. C. Riviere (1971), Nucl.Fusion 11, 363.
22. E. M. Jones (1977), Culham Laboratory Report, CLM-R175.
23. K. T. Dolder and B. Peart (1976), Reports on Progress in Physics 39, 697.
24. G. H. Dunn (1966), J.Chem.Phys. 44, 2592.
25. M. Shimada, M. Nagami, K. Ioki, S. Izumi, M. Maeno, H. Yokomizo, K. Shinya, H. Yoshida, N. H. Brooks, C. L. Hsieh, A. Kitsunozaki and N. Fujisawa (1981), in: "Japanese contributions to the 3rd meeting of the INTOR Phase IIA workshop" IAEA Vienna (Euratom, EURFUBRU/XII-2/81/EDV71, Brussels, 1982).
26. V. A. Abramov (1982), in: "USSR contributions to the 5th meeting of the INTOR Phase IIA workshop" IAEA Vienna (Euratom, EURFUBRU/XII-132/82/EDV23, Brussels, 1982).
27. H. P. Summers and R. W. P. McWhirter (1979), J.Phys.B. 14, 2287.
28. A. Gibson (1978), J.Nucl.Mater. 73/77, 92.
29. M. L. Watkins, A. E. P. M. Abels van Maanen and P. M. Stubberfield (1982), in: "Plasma Physics and Controlled Nuclear Fusion Research (Proc. 9th Int. Conf. Baltimore, 1982) Paper D-2-1.
30. J. Neuhauser, K. Lackner and R. Wunderlich (1982) in: "European contributions to the 5th meeting of the INTOR Phase IIA workshop", IAEA Vienna (Euratom, EURFUBRU/XII-132/82/EDV20, Brussels, 1982).

